Separation and Identification of Dominant Mechanisms in Double Photoionization

Tobias Schneider,* Peter Leszek Chocian,† and Jan-Michael Rost‡

Max Planck Institute for the Physics of Complex Systems, Nöthnitzer Straße 38, 01187 Dresden, Germany

(Received 27 April 2002; published 30 July 2002)

Double photoionization by a single photon is often discussed in terms of two contributing mechanisms, *knockout* (two-step-one) and *shakeoff,* with the latter being a pure quantum effect. It is shown that a quasiclassical description of knockout and a simple quantum calculation of shakeoff provides a clear separation of the mechanisms and facilitates their calculation considerably. The relevance of each mechanism at different photon energies is quantified for helium. Photoionization ratios, integral, and singly differential cross sections obtained by us are in excellent agreement with benchmark experimental data and recent theoretical results.

DOI: 10.1103/PhysRevLett.89.073002 PACS numbers: 32.80.Fb, 03.65.Sq, 34.80.Dp

Our understanding of dynamical processes often rests on isolating approximate mechanisms which leave characteristic traces in the measured or computed observables. A prime example is double photoionization. After the initial absorption of the photon by the primary electron the subsequent redistribution of the energy among the electrons is often discussed in terms of two mechanisms [1,2], knockout (KO) (sometimes called "two-step-one" [3]) and shakeoff (SO) [4–6]. The first mechanism describes the correlated dynamics of the two electrons as they leave the nucleus where the primary electron has knocked out the secondary electron in an $(e, 2e)$-like process. The second mechanism accounts for the fact that absorption of the photon may lead to a sudden removal of the primary electron. This causes a change in the atomic field so that the secondary electron relaxes with a certain probability to an unbound state of the remaining He^+ ion; i.e., the secondary electron is shaken off.

Apart from general properties, e.g., the prevalence of shakeoff at high photon energies, it is difficult to separate the processes. However, they are distinct with respect to their quantum nature: shakeoff is a purely quantum mechanical phenomenon while knockout dynamics occurs classically as well as quantum mechanically. This opens up the possibility to separate shakeoff and knockout by calculating the latter (quasi)classically, provided the quasiclassical approximation to knockout is good. Clearly, the quasiclassical KO mechanism does not contain any part of SO (which is purely quantum).

The two phases of double photoionization, initial absorption and redistribution of the energy, can be expressed by the relation

$$\sigma_X^{++} = \sigma_{\rm abs} P_X^{++}, \tag{1}$$

where X stands for either shakeoff or knockout. In the following, we evaluate P_X^{++} for full fragmentation of the ground state and use the experimental data of Samson *et al.* [7] for $\sigma_{\rm abs}$. We obtain the classical double escape probability for KO with a classical-trajectory Monte Carlo (CTMC) phase space method. CTMC has been frequently used for particle impact induced fragmentation [8–11] with implementations differing typically in the way the phase space distribution $\rho(\Gamma)$ of the initial state is constructed. Details of our approach will be published elsewhere; here we summarize the important steps only.

Within our phase space approach, the double escape probability $P_{\rm KO}^{++}$ is formally given by

$$P_{\rm KO}^{++} = \lim_{t\to\infty} \int d\Gamma_{\mathcal{P}^{++}} \exp[(t - t_{\rm abs})\mathcal{L}_{\rm cl}]\rho(\Gamma), \tag{2}$$

with the classical Liouvillian $\mathcal{L}_{\rm cl}$ for the full three-body Coulomb system propagated from the time $t_{\rm abs}$ of photoabsorption. The projector $\mathcal{P}^{++}$ indicates that we have to integrate over only those parts of phase space that lead to double escape (the asymptotic final energies of the two electrons, ε and $E - \varepsilon$, are positive). The integral in Eq. (2) is evaluated with a standard Monte Carlo technique which entails following classical trajectories in phase space.

The electrons are described immediately after absorption by the distribution

$$\rho(\Gamma) = \mathcal{N}\delta(\vec{r}_1)\rho_2(\vec{r}_2, \vec{p}_2), \tag{3}$$

where $\mathcal{N}$ is a normalization constant. The primary electron absorbs the photon which has an energy $\hbar\omega$. With $\delta(\vec{r}_1)$ we demand the absorption to occur at the nucleus [2], an approximation which becomes exact in the limit of high photon energy [12]. This approximation significantly reduces the initial phase space volume to be sampled. Regularized coordinates [13,14] are used to avoid problems with electron trajectories starting at the nucleus ($\vec{r}_1 = 0$).

The function $\rho_2(\vec{r}_2, \vec{p}_2)$ describing the secondary electron in Eq. (3) is given by

$$\rho_2(\vec{r}_2, \vec{p}_2) = \mathcal{W}_\psi(\vec{r}_2, \vec{p}_2)\delta(\varepsilon_2^{\rm in} - \varepsilon_B). \tag{4}$$

It is obtained by calculating the Wigner distribution, $\mathcal{W}_\psi(\vec{r}_2, \vec{p}_2)$, of the orbital $\psi(\vec{r}_2) = \Psi_0(\vec{r}_1 = 0, \vec{r}_2)$ for a choice of initial wave function Ψ_0 and restricting the initial energy of the secondary electron, $\varepsilon_2^{\rm in}$, to an energy shell ε_B. In the KO mechanism the initial state correlation is not important, so we take the independent particle wave function $\Psi_0(\vec{r}_1, \vec{r}_2) = (Z_{\rm eff}^3/\pi)\exp[-Z_{\rm eff}(\vec{r}_1 + \vec{r}_2)]$ with effective

charge $Z_{\rm eff} = Z - 5/16$. From this choice follows $\varepsilon_B = -Z_{\rm eff}^2/2$ and $\varepsilon_2^{\rm in} = p_2^2/2 - Z_{\rm eff}/r_2$.

The double-to-single ratio in the absence of the SO mechanism is simply given by

$$R_{\rm KO} = P_{\rm KO}^{++}/(1 - P_{\rm KO}^{++}). \tag{5}$$

In Fig. 1 we show $R_{\rm KO}$ as a function of the excess energy E (dashed line). The shape is characteristic of an impact ionization process [16]. For high energies the primary electron moves away so quickly that there is no time to transfer energy to the secondary electron; $R_{\rm KO}$ thus drops to zero as expected. The nonzero asymptotic ratio (indicated by an arrow in Fig. 1) is due to SO which we describe next.

In contrast to KO the shake mechanism is inherently nonclassical in nature. Moreover, initial state correlations are important for shakeoff. As a generalization of the standard formula for SO [5], Åberg gave an expression for the probability to find the shake electron in state ϕ_α at any excess energy [6],

$$P_\alpha^\nu = |\langle \phi_\alpha \mid \psi^\nu \rangle|^2 / \langle \psi^\nu \mid \psi^\nu \rangle, \tag{6}$$

with

$$\psi^\nu(\vec{r}_2) = \int d^3 r_1 \nu^*(\vec{r}_1) \Psi_0(\vec{r}_1, \vec{r}_2), \tag{7}$$

where $\nu(\vec{r}_1)$ is the wave function of the primary electron after it has left the atom. If it was in an s state before the absorption, it is in a p state afterward. The secondary (shake) electron does not change its angular momentum. It can be found with probability P_α in a hydrogenic eigenstate of the bare nucleus, being either bound ($\alpha = n_2$) or in the continuum ($\alpha = \varepsilon$). As for KO, we assume that the primary electron absorbs the photon at the nucleus. In this situation we do not need to know $\nu(\vec{r}_1)$ but can simply replace $\psi^\nu(\vec{r}_2)$ by $\Psi_0(\vec{r}_1 = 0, \vec{r}_2)$ in Eq. (7). We may further simplify the calculation of shakeoff for practical applications in two-electron atoms by taking for $\Psi_0(\vec{r}_1 = 0, \vec{r}_2)$ a normalized hydrogenic wave function $\phi_{1s}^{Z_{\rm SO}}(\vec{r}_2)$ where the correlations have been "absorbed" into an effective shake charge $Z_{\rm SO}$ [17]. For $Z_{\rm SO} \approx 2 - 0.51$ the exact asymptotic ratio $R_\infty = 0.016\,45$ [18,19] is reproduced. We have found little difference for the shake probability as a function of excess energy between this simple ansatz and a fully correlated Hylleraas wave function [20] for Ψ_0.

The shakeoff probability of Eq. (6) reduces now to

$$P_\alpha = |\langle \phi_\alpha \mid \phi^{Z_{\rm SO}} \rangle|^2. \tag{8}$$

The total double ionization probability from shakeoff at finite energies E is given by integrating expression (8) over the energy ε of the shake electron in the continuum ($\alpha \equiv \varepsilon$),

$$P_{\rm SO}^{++}(E) = \int_0^E d\varepsilon \, P_\varepsilon. \tag{9}$$

The photoionization ratio when *only* the SO mechanism is taken into account [same as Eq. (5) but for SO] is shown in Fig. 1 (dot-dashed line). The ratio rises slower than the KO mechanism result, up to an energy of about 100 eV where the KO ratio reaches its maximum value. The SO ratio continues to rise until at a couple of hundred eV it moves more slowly up toward the asymptotic value. An interesting feature of the plot is where the KO and SO results cross at an excess energy of ~350 eV.

To obtain more insight into the two mechanisms, we calculate the differential probabilities $dP_X^{++}/d\varepsilon$, where X stands for either SO or KO. In our classical model of the KO mechanism, we divide the interval of values for ε which corresponds to double escape ($0 \le \varepsilon \le E$) into N equally sized bins (we take $N = 21$) and work out the differential probability by finding the trajectories which

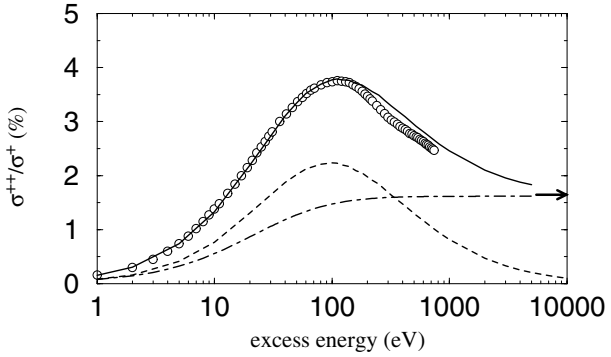

FIG. 1. Photoionization double-to-single ratio. Circles: benchmark experimental data (Samson *et al.* [15]). Full line: complete theoretical result. Dashed line: knockout mechanism only. Dot-dashed line: shakeoff mechanism only. The arrow indicates the asymptotic ratio (~ 1.645%).

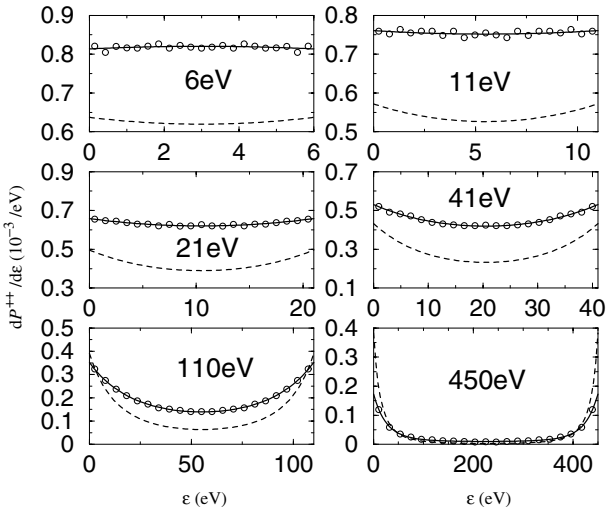

FIG. 2. Differential probabilities for separate knockout and shakeoff mechanisms for a number of excess energies. Circles: knockout mechanism results from binning. Solid lines: fits through circles. Dashed lines: shakeoff mechanism results. See text for details.

fall into the bins. For the SO mechanism the probability per energy unit, P_ε in Eq. (9), already gives the differential probability. Since the electrons are indistinguishable, the differential probabilities must be symmetrized about the equal energy sharing point ($\varepsilon = E - \varepsilon = E/2$),

$$\left.\frac{dP_X^{++}}{d\varepsilon}\right|_{\text{sym}} = \frac{1}{2}\left(\frac{dP_X^{++}(\varepsilon, E)}{d\varepsilon} + \frac{dP_X^{++}(E-\varepsilon, E)}{d\varepsilon}\right). \quad (10)$$

In the case of low excess energy (6 eV), we find a slightly concave shape for the KO distribution (see Fig. 2). This implies a preference for equal energy sharing, the typical behavior close to threshold [21]. The SO result in contrast displays a slightly convex shape which becomes flat as $E \to +0$. Unequal energy sharing is always preferred by SO since the photoelectron is fast with respect to the secondary electron. For all higher excess energies shown, both mechanisms display a convex form.

SO may be viewed as an additional quantum contribution to the quasiclassically calculated double photoionization given by KO. This means that the full result is given by

$$\frac{d\sigma^{++}}{d\varepsilon} = \sigma_{\text{abs}}\left(\frac{dP_{\text{KO}}^{++}}{d\varepsilon} + \frac{dP_{\text{SO}}^{++}}{d\varepsilon}\right). \quad (11)$$

Integration over ε yields the total double ionization cross section,

$$\sigma^{++} = \sigma_{\text{abs}}(P_{\text{KO}}^{++} + P_{\text{SO}}^{++}) \equiv \sigma_{\text{KO}}^{++} + \sigma_{\text{SO}}^{++}. \quad (12)$$

The single ionization cross section is $\sigma^{+} = \sigma_{\text{abs}} - \sigma^{++}$ and the double-to-single ratio is given by $R = \sigma^{++}/\sigma^{+} = P^{++}/(1 - P^{++})$, where $P^{++} = P_{\text{KO}}^{++} + P_{\text{SO}}^{++}$.

In Fig. 1 we compare the ratio R (solid line) to the experimental data of Samson *et al.* [15]. For excess energies up to 200 eV we find an excellent agreement. In the energy regime where the two contributions are of the same size there is a deviation between experiment and our result (at worst 8%). Exactly in this situation any interference which exists between SO and KO would show its largest effect. The deviation we find may be due to such an interference which we cannot account for since we determine KO quasiclassically. At higher energies the difference decreases again (already visible in the plot) until at very high energies our result reproduces the asymptotic ratio.

From the agreement with the experiment, we can infer that interference between SO and KO is in general small. As one can also conclude from [1], this is probably a consequence of the fact that the fully differential ionization amplitudes (which should be added coherently) are very different for SO and KO. The issue can be clarified with the formulation of SO and KO differential in the angles. This is planned and possible, although it will require considerably more numerical effort to obtain KO with sufficient statistics in the CTMC calculation.

Here we can assess the relative importance of both contributions to the single differential cross section (energy sharing) at different total energies E. From Fig. 2 one sees that at 110 eV SO has become more important than KO for highly unequal energy sharings. As energy is increased to 450 eV, SO begins to dominate regions of unequal energy sharing. On the other hand, KO is higher at equal energy sharing for all excess energies E.

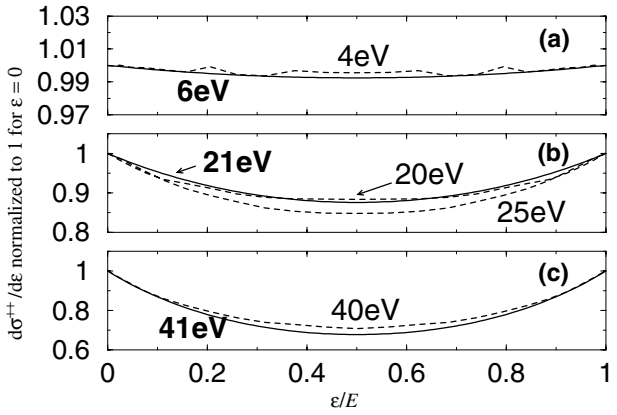

FIG. 3. Singly differential cross sections normalized to 1 for $\varepsilon = 0$. Solid lines: our complete theoretical results at excess energies of (a) 6, (b) 21, and (c) 41 eV. Dashed lines: new results of Colgan *et al.* [22] at excess energies of (a) 4, (b) 20 and 25, and (c) 40 eV.

Figure 3 shows that our singly differential cross sections (SDCS) agree well with the recent *ab initio* theoretical results of Colgan *et al.* [22]. We note that the results of Proulx and Shakeshaft [23] show a concave shape for

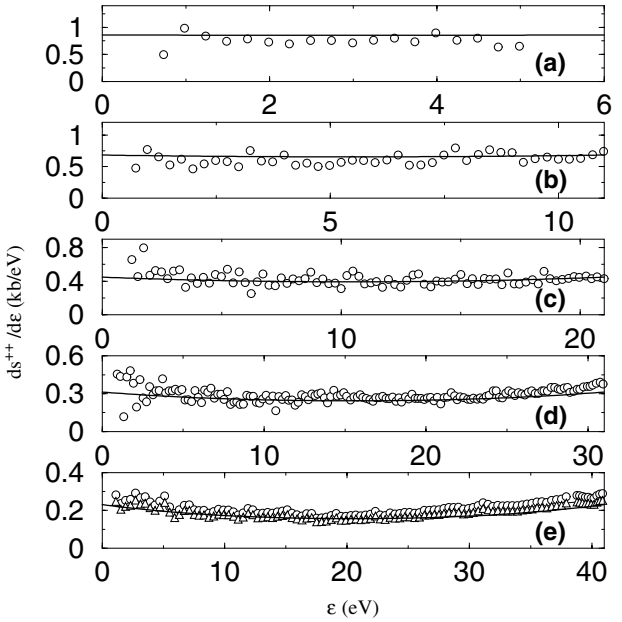

FIG. 4. Absolute singly differential cross sections. Solid lines: our theoretical results at excess energies of (a) 6, (b) 11, (c) 21, (d) 31, and (e) 41 eV. Circles: recalibrated (see text) experimental data of Wehlitz *et al.* [24] at the same excess energies apart from (a) which is at 5 eV. The triangles in (e) additionally show the Wehlitz data renormalized to the σ^{++}(41 eV) of Samson [15].

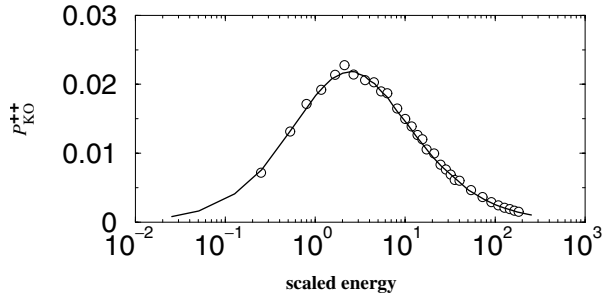

FIG. 5. P^{2+}_{KO} (solid line) as a function of the scaled energy E/E'_B compared to the cross section for electron impact ionization of He^+ [27] (circles) as a function of E/E_B (see text). Additionally, the impact ionization data has been multiplied by a factor $C = 4.67 \times 10^{15}$ cm^{-2} to make the maxima of both curves the same height. ($1/C$ may be interpreted as the geometric cross section.)

excess energies below 20 eV. This is in disagreement with our results which are convex down to 6 eV. In Fig. 4 we compare our absolute SDCS to the experimental data of Wehlitz *et al.* [24], which has been recalibrated using the values of the photoabsorption cross section of Samson *et al.* [7]. In their original work, Wehlitz *et al.* normalized their SDCS using a photoabsorption cross section [25] which is now known to overestimate the 5–41 eV range by 9% to 16%. In addition, the photoionization ratio they measured at 41 eV is ~17% higher than the Samson *et al.* [15] data, and so we renormalize Fig. 4(e) to take this into account.

Our approach not only facilitates the calculation of double photoionization, it also offers considerable insight into the physical process, e.g., concerning the similarity with electron impact ionization of He^+ [2,26]. Indeed, we can show that impact ionization may be viewed as the KO part of double photoionization (Fig. 5). The only difference is that impact ionization sees a He^+ hydrogenic target electron with binding energy $E_B = -Z^2/2, Z = 2$, while the KO process involves a bound electron with energy $E'_B = -Z^2_{\mathrm{eff}}/2$. One may thus say that both processes differ only slightly, namely, in the energy scale set by the respective bound electron.

We conclude that the separate formulation and calculation of knockout and shakeoff offers an accurate description of double photoionization. Interestingly, this implies little interference between both contributions, a fact which deserves further study in the future. Because of the moderate numerical effort required, our approach can be extended along two directions: first, to describe angular differential cross sections for double ionization and second, to describe total and energy resolved triple photoionization cross sections.

It is a pleasure to thank R. Wehlitz and J. Colgan for providing us with their results. T. S. thanks Andreas Becker and Thomas Pattard for valuable discussions. Financial support by the DFG within the Gerhard Hess-program is gratefully acknowledged.

*Electronic address: tosch@mpipks-dresden.mpg.de
†Electronic address: pete@spymac.com
‡Electronic address: rost@mpipks-dresden.mpg.de

[1] A. Knapp *et al.*, Phys. Rev. Lett. (to be published).
[2] T. Pattard and J. Burgdörfer, Phys. Rev. A **64**, 042720 (2001).
[3] J. A. Tanis *et al.*, Phys. Rev. Lett. **83**, 1131 (1999).
[4] F. Bloch, Phys. Rev. **48**, 187 (1935).
[5] A. Dalgarno and A. L. Stewart, Proc. Phys. Soc. London **76**, 49 (1960).
[6] T. Åberg, Ann. Acad. Sci. Fenn., Ser. A6 **308**, 1 (1969); Phys. Rev. A **2**, 1726 (1970).
[7] J. A. R. Samson, Z. X. He, L. Yin, and G. N. Haddad, J. Phys. B **27**, 887 (1994).
[8] R. Abrines and I. C. Percival, Proc. Phys. Soc. London **88**, 861 (1966).
[9] D. J. W. Hardie and R. E. Olson, J. Phys. B **16**, 1983 (1983).
[10] D. Eichenauer, N. Grün, and W. Scheid, J. Phys. B **14**, 3929 (1981).
[11] J. S. Cohen, J. Phys. B **18**, 1759 (1985).
[12] P. K. Kabir and E. E. Salpeter, Phys. Rev. **108**, 1256 (1957).
[13] P. Kustaanheimo and E. Stiefel, J. Reine Angew. Math. **218**, 204 (1965).
[14] S. J. Aarseth and K. Zare, Celest. Mech. **10**, 185 (1974).
[15] J. A. R. Samson, W. C. Stolte, Z.-X. He, J. N. Cutler, and Y. Lu, Phys. Rev. A **57**, 1906 (1998).
[16] J.-M. Rost and T. Pattard, Phys. Rev. A **55**, R5 (1997).
[17] T. Surić, K. Pisk, and R. H. Pratt, Phys. Lett. A **211**, 289 (1996).
[18] R. C. Forrey, H. R. Sadeghpour, J. D. Baker, J. D. Morgan, and A. Dalgarno, Phys. Rev. A **51**, 2112 (1995).
[19] R. Krivec, M. Y. Amusia, and V. B. Mandelzweig, Phys. Rev. A **62**, 064701 (2000).
[20] A. L. Stewart and T. G. Webb, Proc. Phys. Soc. London **82**, 532 (1963).
[21] J.-M. Rost, Phys. Rev. Lett. **72**, 1998 (1994).
[22] J. Colgan, M. S. Pindzola, and F. Robicheaux, J. Phys. B **34**, L457 (2001); J. Colgan and M. S. Pindzola, Phys. Rev. A **65**, 032729 (2002).
[23] D. Proulx and R. Shakeshaft, Phys. Rev. A **48**, R875 (1993).
[24] R. Wehlitz, F. Heiser, O. Hemmers, B. Langer, A. Menzel, and U. Becker, Phys. Rev. Lett. **67**, 3764 (1991).
[25] G. V. Marr and J. B. West, At. Data Nucl. Data Tables **18**, 497 (1976).
[26] J. A. R. Samson, Phys. Rev. Lett. **65**, 2861 (1990); J. A. R. Samson, R. J. Bartlett, and Z. X. He, Phys. Rev. A **46**, 7277 (1992).
[27] A. B. Peart, D. S. Walton, and K. T. Dolder, J. Phys. B **2**, 1347 (1969).